dc spin current generation in a Rashba-type quantum channel

L. Y. Wang,[1] C. S. Tang,[2] and C. S. Chu[1]
[1]*Department of Electrophysics, National Chiao Tung University, Hsinchu 30010, Taiwan*
[2]*Physics Division, National Center for Theoretical Sciences, P.O. Box 2-131, Hsinchu 30013, Taiwan*
(Received 15 August 2005; revised manuscript received 2 November 2005; published 2 February 2006)

We propose and demonstrate theoretically that resonant inelastic scattering (RIS) can play an important role in dc spin current generation. The RIS makes it possible to generate dc spin current via a simple gate configuration: a single finger gate that locates atop and orients transversely to a quantum channel in the presence of Rashba spin-orbit interaction. The ac-biased finger gate gives rise to a time variation in the Rashba coupling parameter, which causes spin-resolved RIS and, subsequently, contributes to the dc spin current. The spin current depends on both the static and the dynamic parts in the Rashba coupling parameter, α_0 and α_1, respectively, and is proportional to $\alpha_0\alpha_1^2$. The proposed gate configuration has the added advantage that no dc charge current is generated. Our study also shows that the spin current generation can be enhanced significantly in a double finger-gate configuration.

DOI: 10.1103/PhysRevB.73.085304 PACS number(s): 73.23.−b, 72.25.−b, 72.30.+q

I. INTRODUCTION

Spintronics is important in both application and fundamental arenas.[1,2] A recent key issue of great interest is the generation of dc spin current (SC) without charge current. Various dc SC generation schemes have been proposed, involving static magnetic field,[3–5] ferromagnetic material,[6] or ac magnetic field.[7] More recently, Rashba-type spin-orbit interaction (SOI) in two dimension electron gas (2DEG)[8–10] has inspired attractive proposals for nonmagnetic dc SC generation.[11–13] Of these recent proposals, including a time-modulated quantum dot with a static spin-orbit coupling,[11] and time modulations of a barrier and the spin-orbit coupling parameter in two spatially separated regions,[12] the working principle is basically adiabatic quantum pumping. Hence, simultaneous generation of both dc spin and charge current is the norm. The condition of zero dc charge current, however, is met only for some judicious choices for the values of the system parameters.

It is known, on the other hand, that quantum transport in a narrow channel exhibits resonant inelastic scattering (RIS) features when it is acted upon by a spatially localized time-modulated potential.[14,15] This RIS is coherent inelastic scattering, but with resonance at work, when the traversing electrons can make transitions to their subband threshold by emitting $m\hbar\Omega$.[14,15] Should this RIS become spin resolved in a Rashba-type quantum channel (RQC), of which its Rashba coupling parameter is time modulated locally, we will have a simpler route to the nonmagnetic generation of dc SC. Thus, we opt to study, in this work, the RIS features in a RQC. This requires us to go beyond the adiabatic regime and into the regime when either μ or $\mu_n \sim \hbar\Omega$. We solve the time-dependent spin-orbit scattering (SOS) for all possible incident electron energies and obtain large RIS contribution. In the adiabatic regime, however, with μ, $\mu_n \gg \hbar\Omega$, we find that the dc spin-pumping effect from a sole SOI time-modulated region is small.[12]

II. SYSTEM CONFIGURATION

The system configuration considered is based on a RQC that forms out of a 2DEG in an asymmetric quantum well by the split-gate technique. As is depicted in Fig. 1(a), a finger gate (FG) is positioned above while separated from the RQC by an insulating layer. A local time variation in the Rashba coupling parameter $\alpha(\mathbf{r},t)$ can be induced by ac biasing the FG.[12,13] The Hamiltonian is given by $\mathcal{H}=p^2/2m+\mathcal{H}_{so}(\mathbf{r},t)+V_c(y)$ where the Rashba term

$$\mathcal{H}_{so}(\mathbf{r},t)=\mathbf{M}\cdot\tfrac{1}{2}[\alpha(\mathbf{r},t)\boldsymbol{p}+\boldsymbol{p}\alpha(\mathbf{r},t)]. \quad (1)$$

Here, $\mathbf{M}=\hat{\mathbf{z}}\times\boldsymbol{\sigma}$, $\hat{\mathbf{z}}$ is normal to the 2DEG, $\boldsymbol{\sigma}$ is the vector of Pauli spin matrices, and $V_c(y)$ is the confinement potential. The unperturbed Rashba coupling parameter $\alpha(\mathbf{r},t)$ is α_0 throughout the RQC, but becomes $\alpha_0+\alpha_1\cos\Omega t$ in the region underneath the ac-biased FG. The Dresselhaus term is neglected for the case of a narrow-gap semiconductor system.[16]

To demonstrate the pumping mechanism, we consider a narrow RQC in which its subband energy spacing is much greater than the Rashba-induced subband mixing. As such, the unperturbed Hamiltonian, in its dimensionless form, is $\mathcal{H}_0=-\nabla^2+\alpha_0\sigma_y(i\partial/\partial x)+V_c(y)$. Appropriate units have been used such that all physical quantities presented here, and henceforth, are dimensionless.[15] In particular, α is in unit of $v_F^*/2$, and spin in unit of $\hbar/2$. The right-going (R) eigenstate of $\mathcal{H}_0$, in the nth subband, is $\phi_n(y)\psi_n^\sigma(x)$, where $\psi_n^\sigma(x)=\exp[ik_{n,R}^\sigma x]\chi_\sigma$. The wave vector $k_{n,R}^\sigma=\sqrt{\mu_n+\eta_\sigma\alpha_0/2}$,

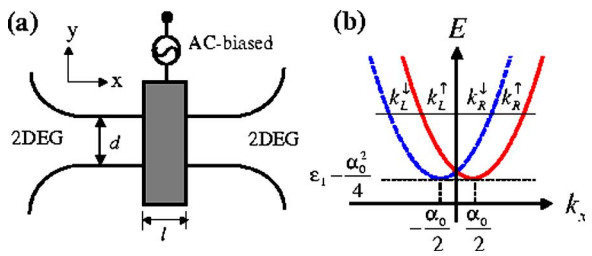

FIG. 1. (Color online) (a) Top-view schematic illustration of the RQC. The ac-biased FG, of width l, is indicated by the gray area; (b) the electron dispersion relation of an unperturbed RQC.

while $\eta_\sigma = \pm 1$ denotes the eigenvalue of χ_σ to the operator σ_y. μ_n is the energy measured from the nth subband threshold such that the energy of the eigentstate is $E = \mu_n + \varepsilon_n - \alpha_0^2/4$, for $\varepsilon_n = (n\pi/d)^2$. This dispersion relation is shown in Fig. 1(b). The subband with $\mu_n \sim \hbar\Omega$ is found to contribute most to the RIS-enhanced spin pumping. It is of import to note that right-going electrons have $|k_R^\uparrow| > |k_R^\downarrow|$ and that, at the subband threshold, $k_R^{\uparrow(\downarrow)} = k_L^{\uparrow(\downarrow)}$.

III. PHYSICAL PICTURE

In this section, we show that the physical origin of the dc SC generation can be understood from two perspectives. A weak pumping regime result is then obtained for an explicit confirmation of our physical reasoning.

The first perspective is associated with the vector potential. In the ac-biased region, $\mathcal{H} = \mathcal{H}_x + \mathcal{H}_y$, the transverse part $\mathcal{H}_y = -\partial^2/\partial y^2 + V_c(y)$, and the longitudinal part

$$\mathcal{H}_x(t) = \left(-i\frac{\partial}{\partial x} + \frac{\alpha(x,t)}{2}\mathbf{M}\cdot\hat{\boldsymbol{x}} \right)^2 - \frac{1}{4}\alpha(x,t)^2. \tag{2}$$

The form of Eq. (2) suggests an effective vector potential, $\mathbf{A}(t) = \frac{1}{2}\alpha(x,t)\mathbf{M}\cdot\hat{\boldsymbol{x}}$, which depends on the spin and gives rise to a spin-resolved driving electric field $\mathbf{E} = -\partial\mathbf{A}/\partial t$. However, in $\mathcal{H}_x$, the A^2 term does not depend on $\boldsymbol{\sigma}$, while for the term linear in $\mathbf{A}$, $\mathbf{A}\chi_\sigma = -\frac{1}{2}\eta_\sigma\alpha(x,t)\chi_\sigma$ gives rise only to a trivial spin dependence, which can be easily removed by a shift in the origin of time for the case of an oscillatory $\alpha(x,t)$. Yet it turns out that the full term linear in $\mathbf{A}$, given by $-i(\partial/\partial x)\hat{x}\cdot\mathbf{A}$, manages to give rise to nontrivial spin-resolved transmissions. In a perturbative sense, this term becomes $k_R^{\uparrow(\downarrow)}A_x$, for the case of a right-going electron incident upon a spatially uniform $\alpha(t)$. This renders the effective longitudinal driving field to become spin dependent, through the factor $k_R^{\uparrow(\downarrow)}$. The difference in the current transmissions, for spin-up and spin-down cases, is proportional to the difference in $k_R^{\uparrow(\downarrow)}$, or α_0, and is found to be amplified by RIS. This breaking of the longitudinal symmetry in the effective driving field by α_0 leads to the generation of dc spin current in a FG-RQC structure that has but an apparent longitudinal configuration symmetry, and with zero source-drain bias. No dc charge current will be generated, however, in such a structure.

An alternate perspective for the understanding of the origin of the spin-resolved current transmission is associated with a unitary transformation. By introducing a unitary transformation $\Psi_\sigma(x,t) = \exp[(i\eta_\sigma/2)\int_{-l/2}^{x}\alpha(x',t)dx']\psi_\sigma(x,t)$, the Schrödinger equation [Eq. (2)] becomes

$$\left[-\frac{\partial^2}{\partial x^2} + U_1(t) + U_2^\sigma(t) \right]\psi_\sigma(x,t) = i\frac{\partial}{\partial t}\psi_\sigma(x,t), \tag{3}$$

of which the two time-dependent potentials are $U_1(t) = -\alpha(x,t)^2/4$ and $U_2^\sigma(t) = (\Omega\alpha_1/2)(x+l/2)\cos(\Omega t + \eta_\sigma\pi/2)$. Even though only U_2^σ depends on spin, both the term in $U_1(t)$ that oscillates with frequency Ω and U_2^σ together constitute a pair of quantum pumping potential that pump SC. This is our major finding in this work: that spin pumping nature is built-in even in a single FG configuration.

The SC expression for a state Ψ_σ is given by the SC density operator

$$\hat{J}_x^y = i\left[\frac{\partial\Psi_\sigma^\dagger}{\partial x}\sigma_y\Psi_\sigma - \text{H.c.} \right] + \frac{\alpha}{2}\Psi_\sigma^\dagger\{\sigma_y, \mathbf{M}\}_x\Psi_\sigma. \tag{4}$$

The SC conservation is maintained by the supression of subband mixing and the associated spin-flipping in a RQC. For a scattering state Ψ_σ, the SC can be expressed in terms of the transmission coefficients. More specifically, the ratio between the time-averaged transmitted and the incident SC gives the spin-resolved current transmission $T_{\beta\alpha}^\sigma$, where α, β, are, respectively, the incident and the transmitting lead. Summing over contributions from all states in reservoirs R and L, the SC is

$$I^s = I^\uparrow - I^\downarrow,$$

where

$$I^\sigma = \int dE f(E)[T_{RL}^\sigma - T_{LR}^\sigma], \tag{5}$$

and I^σ is the number current due to electrons with spin η_σ from both reservoirs that are under zero source-drain bias condition. Here $T_{RL}^\sigma = \Sigma_n\Sigma_{m(\mu_n^m>0)}T_{n,RL}^{m,\sigma}$ and $f(E)$ is the Fermi-Dirac distribution. The transmission coefficient $T_{n,RL}^{m,\sigma} = |t_{n,RL}^{m,\sigma}|^2\sqrt{\mu_n^m/\mu_n}$ denotes the current transmission that an electron incident from terminal L in the spin channel σ, subband n, energy E, is scattered into terminal R, sideband m, with kinetic energy $\mu_n^m = \mu_n + m\Omega$. The net charge current is given by $I^q = I^\uparrow + I^\downarrow$. In a symmetric FG configuration, we have $T_{LR}^\sigma = T_{RL}^\sigma$, so that the net spin current is $I^s = 2\int dE f(E)(T_{RL}^\uparrow - T_{RL}^\downarrow)$ and the net charge current is identically zero.

In the weak pumping (WP) regime, when α_1 is small, we can demonstrate analytically, and most unequivocally, that spin-dependent reflection arises merely from the aforementioned linear $\mathbf{A}$ term in $H_x(t)$. We outline the derivation here while leaving the detail in Appendix A. Tracing up to the first order in α_1, our derivation retains the reflection amplitudes to $m = \pm 1$ sideband and drops that to the $m = 0$ sideband. Contribution to the total reflection includes thus reflection at either the left or the right edges of the time-modulated region. For an electron incident from terminal L with wave vector $k_{n,R}^\sigma(E)$, the reflection at the left edge is obtained from the wave-function continuous condition and the boundary condition

$$-\frac{\partial}{\partial x}\Psi_\sigma|_{x=(-l/2)^+} + \frac{\partial}{\partial x}\Psi_\sigma|_{x=(-l/2)^-} + \frac{i}{2}\eta_\sigma\alpha_1\cos\Omega t\,\Psi_\sigma|_{x=-l/2} = 0. \tag{6}$$

In the time-modulated region, the wave function Ψ_σ consists of one-sideband terms, given by the form $e^{ik_{n,R}^\sigma(E\pm\Omega)x}e^{-i(E\pm\Omega)t}$, and the $m = 0$ term, given by the form $e^{ik_{n,R}^\sigma(E)x}e^{-iEt}[1 + \eta_\sigma/(2\Omega)\alpha_1 k_{n,R}^\sigma(E)(e^{i\Omega t} - e^{-i\Omega t})]$. The extra Ωt dependence in the $m = 0$ term is resulted from the time-dependent driving effect of $\mathbf{A}$, which is obviated by the

weighting factor that involves $\alpha_1 k^{\sigma}_{n,R}$. The reflection amplitude $r^{m,\sigma}_L$ at the left edge is obtained to be

$$r^{m,\sigma}_L = \mathrm{sgn}(m)\frac{\eta_\sigma}{2}\frac{\left[\frac{\alpha_1}{\Omega}k^{\sigma}_{n,R}(k^{\sigma}_{n,R}-k^{m,\sigma}_{n,R})+\frac{\alpha_1 m}{2}\right]}{k^{m,\sigma}_{n,R}-k^{m,\sigma}_{n,L}} \times e^{-i(k^{\sigma}_{n,R}-k^{m,\sigma}_{n,L})l/2} \tag{7}$$

for $m=\pm 1$. The first term in the numerator of Eq. (7) is clearly due to **A**, because of the factor $\alpha_1 k^{\sigma}_{n,R}$, and the second term is due to the scattering at the edge. Here the wave vector $k^{m,\sigma}_{n,R(L)}=\pm(\mu^m_n)^{1/2}+\eta_\sigma\alpha_0/2$, with upper (lower) sign corresponds to the right-(left-) moving electron in the nth subband, mth sideband, and with kinetic energy μ^m_n. It is clear then that wave-vector differences in both the numerator and the denominator of $r^{m,\sigma}_L$ are spin independent. Hence, the spin dependence arises solely from the $\alpha_1 k^{\sigma}_{n,R}$ factor in the first term of the numerator in Eq. (7), or from **A**. This confirms our understanding of the physical origin of the dc SC generation.

Including the reflection at the right edge, we obtain the total reflection amplitude

$$r^{m,\sigma}_{n,LL}=[1-e^{i(k^{\sigma}_{n,R}-k^{m,\sigma}_{n,L})l}]r^{m,\sigma}_L. \tag{8}$$

We note that the spin dependence of this total reflection amplitude is associated with α_0. In fact, it turns out that the SC is proportional to α_0. The SC is related to the current transmission, which, within the aforementioned approximation, is given by $T^{\sigma}_{RL}\approx 1-\Sigma_n[R^{1,\sigma}_{n,LL}+R^{-1,\sigma}_{n,LL}]$, where $R^{m,\sigma}_{n,LL}=|r^{m,\sigma}_{n,LL}|^2\sqrt{\mu^m_n}/\sqrt{\mu_n}$. From Eq. (5), the energy derivative of the zero-temperature SC is given by $\partial I^s/\partial E=2\Delta T_{RL}=2(T^{\uparrow}_{RL}-T^{\downarrow}_{RL})$ from which its explicit expression is given by

$$\frac{\partial I^s}{\partial E}=\frac{1}{2}\alpha_0\alpha_1^2\sum_n\sum_{\substack{m=\pm 1\\(\mu^m_n>0)}}\frac{\{1-\cos[(\sqrt{\mu_n}+\sqrt{\mu^m_n})l]\}\left[\left(\frac{1}{4}\right)^2-\left(\frac{1}{\Omega}(\mu_n-\sqrt{\mu_n\mu^m_n})+\frac{m}{4}\right)^2\right]}{\mu_n\sqrt{\mu^m_n}}. \tag{9}$$

That this expression diverges when $\mu^m_n=0$, for $m<0$, exhibits the RIS feature unambiguously and also demonstrates the need to go beyond the one-sideband approximation near the RIS condition.

IV. NUMERICAL RESULTS AND DISCUSSIONS

In the following, we present results obtained from solving the time-dependent SOS exactly, in the numerical sense. An outline of the method is presented in Appendix B. Physical parameters are chosen to be consistent with the InGaAs-InAlAs–based narrow-gap heterostructures such that the electron density $n_e=1\times 10^{12}\ \mathrm{cm}^{-2}$, effective mass $m^*=0.04m_0$, and $\alpha_0=0.13$ ($\hbar\alpha_0=3\times 10^{-11}$ eV m).[9] Accordingly, the length unit $l^*=4.0$ nm and the energy unit $E^*=59$ meV.

For the case of one FG ($N=1$), the energy dependence of the spin-resolved transmission T^{σ}_{RL} is plotted in Figs. 2(a)–2(c), and that of the corresponding dc SC is plotted in Fig. 2(d). The FG width $l=20$ (80 nm), driving frequency $\Omega=0.002$ ($\nu=\Omega/2\pi\approx 28$ GHz), and energy $\mu=E-\varepsilon_1$. Dip features in T^{σ}_{RL} at $\mu/\Omega=1$ are the quasi-bound state (QBS) features, where electrons undergo coherent inelastic scattering to a QBS just beneath its subband bottom.[14] Higher-order QBS features at $\mu/\Omega=2$ are barely shown by the small peaks. Of particular interest is the change in sign in the transmission difference $\Delta T_{RL}=T^{\uparrow}_{RL}-T^{\downarrow}_{RL}$ across the dip structures, namely, $\Delta T_{RL}(\mu=\Omega^-)>0$ while $\Delta T_{RL}(\mu=\Omega^+)<0$. This leads to a nonzero dc SC, peaked at $\mu/\Omega=1$, and is exhibited in Fig. 2(d).

It is also shown that the dc SC increases with the oscillating amplitude α_1 of the ac-biased gate voltage. More importantly, all the above dc SC characteristics, including even their order of magnitudes, are already captured by Eq. (9). This lends strong support to our finding that RIS has played a pivotal role in the generation of dc SC. Similar RIS-induced peak in I^s is found if we vary d instead of μ.

The nonlinear enhancement in the dc SC by two FGs ($N=2$) is presented in Figs. 3(a)–3(c). The driving frequency

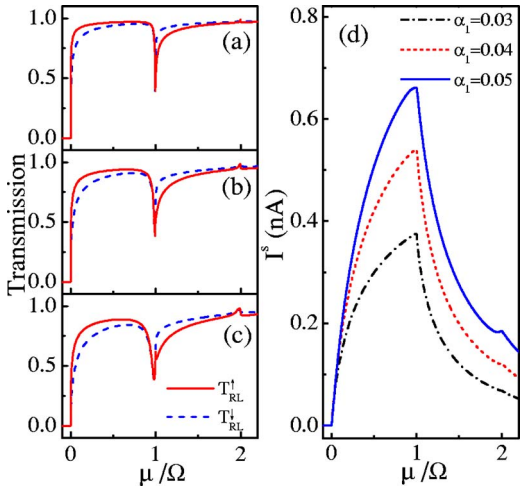

FIG. 2. (Color online) Spin-resolved current transmissions $T^{\uparrow}_{RL}$ (solid) and $T^{\downarrow}_{RL}$ (dashed) versus the incident energy μ/Ω. Parameters $N=1$, $\alpha_0=0.13$, $\Omega=0.002$, $l=20$, and $\alpha_1=$(a) 0.03, (b) 0.04, and (c) 0.05. The corresponding dc SC is plotted in (d).

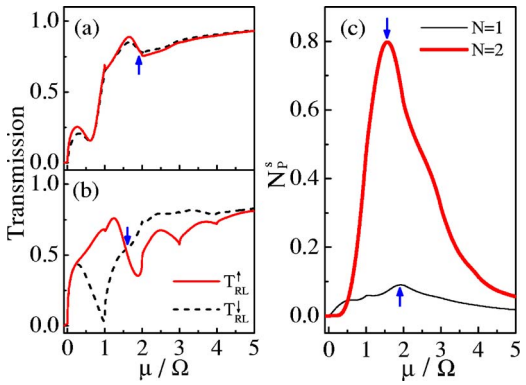

FIG. 3. (Color online) Current transmission versus μ/Ω for N=(a) 1, and (b) 2. Pumped spins per cycle are plotted in (c) for N=1 (thick curve) and N=2 (thin curve) with α_1=0.065, and driving frequency Ω=0.001. Other parameters are the same as in Fig. 2.

is chosen to be Ω=0.001 ($\nu \approx 14$ GHz), and with l=22 ($\simeq$88 nm). For comparison, the N=1 FG transmissions are plotted along with that of the N=2 FG case, in Figs. 3(a) and 3(b), respectively. The corresponding dc SC, expressed in terms of pumped spins per cycle $N_P^s=(2\pi/\Omega)|I^s|$, is shown in Fig. 3(c). The pumping is optimized by a choice of the FG separation, with the edge-to-edge separation Δl=22. The QBS dip structures are significant up to the fourth sideband in Fig. 3(b). As indicated by arrows, the pumped spin-per-cycle peaks at $\mu/\Omega \simeq 1.57$ (1.92), with peak value 0.8 (0.1) for the N=2 (N=1) FG case. The enhancement in N_P^s is far greater than doubling the N_P^s of N=1 FG. Finally, we discuss the effectiveness of tuning α. Grundler showed that a static FG bias change $\Delta V_{\rm FG} \sim 0.075$ V can tune $\Delta\alpha \sim 0.25\alpha_0$.[10] This tuning ability should remain valid in ac FG bias if the wave function in the asymmetric quantum well responses adiabatically. We estimate the quantum-well energy-level spacing $\Delta E \sim 0.08$ eV $\gg \hbar\Omega \sim 0.06$ meV, for $\Omega/(2\pi)$=14 GHz. Thus, the adiabatic response of the wave function in the quantum well is established. Furthermore, the ac FG biases, with amplitude $\Delta V_{\rm FG} \sim 0.075$ V, is estimated to be within reach of coaxiable cable technology.[17]

V. CONCLUSION

In conclusion, a nonmagnetic way of generating dc SC has been established. The proposed Rashba-type quantum channel driven by an ac-biased finger gate is a simple structure and should be within reach of recent fabrication capability. The spin pumping is studied, in detail, in both its nature and its pumping mechanism. A resonant inelastic process is the major factor that contributes to the robustness of the spin pumping. The coherent nature of the pumping supports further enhancement of the spin pumping by invoking configuration consisting of more than one finger gate.

ACKNOWLEDGMENTS

The authors acknowledge valuable discussions with A. G. Mal'shukov. This work was funded by the National Science Council of ROC under Grants No. NSC92-2112-M-009-035, No. NSC92-2120-M-009-010, No. NSC93-2112-M-009-036, and No. NSC93-2119-M-007-002 (NCTS).

APPENDIX A: WEAK-PUMPING (WP) REGIME

In the WP regime, we can obtain analytic results. The WP regime refers to the case when the Rashba coupling parameter oscillates with a small amplitude α_1. Keeping only up to the lowest nonvanishing contribution of α_1, it is simpler to calculate the reflection amplitudes than the transmission coefficients. The reflection amplitudes to $m=\pm 1$ sidebands are first order in α_1 and are the major objects of our calculation here. The reflection amplitudes to m=0 sideband, however, is second order in α_1 and is neglected. When the Rashba coupling parameter oscillates in time within a spatial region $-l/2<x<l/2$, the longitudinal Hamiltonian is given by

$$H_x = -\frac{\partial^2}{\partial x^2} + \alpha_0\sigma_y\left(i\frac{\partial}{\partial x}\right) + \frac{\alpha_1\cos\Omega t}{2}\sigma_y \times\left[\theta(l/2-|x|)\left(i\frac{\partial}{\partial x}\right)+\left(i\frac{\partial}{\partial x}\right)\theta(l/2-|x|)\right], \quad \text{(A1)}$$

where $\theta(x)$ is the step function. For an electron incident from terminal L with wave vector $k_{n,R}^{\sigma}(E)$, the reflection coefficients consist of contributions from reflections at the left and the right edges of the time-modulated region. We first calculate the reflection amplitudes due to reflection at $x=-l/2$. The wave function is given by

$$\psi_n^{\sigma}(x<-l/2) = e^{ik_{n,R}^{\sigma}(E)x}e^{-iEt} + \sum_{\substack{m=\pm 1\\(m\neq 0)}} r_L^{m,\sigma}e^{ik_{n,L}^{m,\sigma}x}e^{-i(E+m\Omega)t}, \quad \text{(A2)}$$

$$\psi_n^{\sigma}(-l/2<x<l/2) = \sum_{\substack{m=\pm 1\\(m\neq 0)}} t_L^{m,\sigma}e^{ik_{n,R}^{m,\sigma}x}e^{-i(E+m\Omega)t} + t_L^{0,\sigma}e^{ik_{n,R}^{\sigma}(E)x}e^{-iEt}\left[1+\frac{\eta_\sigma}{2\Omega}\alpha_1 k_{n,R}^{\sigma}(E)(e^{i\Omega t}-e^{-i\Omega t})\right]. \quad \text{(A3)}$$

Here, $t_L^{m,\sigma}$ and $r_L^{m,\sigma}$ denote, respectively, the transmission and reflection coefficients at the left edge of the time-modulated region. We have not included, in Eq. (A3), corrections to the wave functions associated with the coefficients $t_L^{m,\sigma}$, for $m=\pm 1$, that arise from the time-modulation of the Rashba spin-orbit intraction (SOI). It is because the coefficients $t_L^{m,\sigma}$ are already first order in α_1. These coefficients are solved from the wave-function continuous condition and the boundary condition in Eq. (6). The reflection coefficients are calculated, and the expression is presented in Eq. (7). It is worth noting that $t_L^{0,\sigma}=1$, up to first order in α_1.

Following a similar procedure, the reflection at the right edge of the time-modulated region can be obtained from the following wave function:

$$\psi_n^\sigma(-l/2<x<l/2) = e^{ik_{n,R}^\sigma(E)x}e^{-iEt}\left[1+\frac{\eta_\sigma\alpha_1}{2\Omega}k_{n,R}^\sigma(E)(e^{i\Omega t}-e^{-i\Omega t})\right] + \sum_{m=0,\pm1} r_R^{m,\sigma}e^{ik_{n,L}^{m,\sigma}x}e^{-i(E+m\Omega)t} \times\left[1+\frac{\eta_\sigma\alpha_1}{2\Omega}k_{n,L}^{m,\sigma}(e^{i\Omega t}-e^{-i\Omega t})\right], \quad \text{(A4)}$$

$$\psi_n^\sigma(x>l/2) = \sum_{m=0,\pm1} t_R^{m,\sigma}e^{ik_{n,R}^{m,\sigma}x}e^{-i(E+m\Omega)t}. \quad \text{(A5)}$$

Again, $t_R^{m,\sigma}$ and $r_R^{m,\sigma}$ denote the transmission and the reflection coefficients, respectively, at the right edge of the time-modulated region. It is noted that in Eq. (A4), only one incident wave needs to be considered. The incident waves associated with coefficients $t_L^{m,\sigma}$ in Eq. (A3), for $m=\pm1$, is neglected because these coefficients are, themselves, first order in α_1. Invoking the wave-function continuous condition and the boundary condition

$$\frac{\partial}{\partial x}\psi_n^\sigma|_{x=(l/2)^-} - \frac{\partial}{\partial x}\psi_n^\sigma|_{x=(l/2)^+} - \frac{i}{2}\eta_\sigma\alpha_1\cos\Omega t\,\psi_n^\sigma|_{x=l/2} = 0, \quad \text{(A6)}$$

we obtain

$$r_R^{m,\sigma} = -e^{i(k_{n,R}^\sigma - k_{n,L}^{m,\sigma})l}r_L^{m,\sigma}, \quad \text{(A7)}$$

and the total reflection coefficient, up to the first order in α_1 is given by $r_{n,LL}^{m,\sigma}=r_R^{m,\sigma}+r_L^{m,\sigma}$, for $m=\pm1$, which explicit expression is presented in Eq. (8).

APPENDIX B: FORMULATION FOR NUMERICAL CALCULATION

The Hamiltonian in the ac-biased region, given by Eq. (2), can have its time-modulated term transformed away by the use of a transformation: $\Psi_{n,\sigma}(x,t) = \exp[\eta_\sigma(\alpha_1/\Omega)\sin\Omega t(\partial/\partial x)]\psi_n^\sigma(x)$, where ψ_n^σ satisfies Eq. (2) with α_1 sets to zero. Thus, the general form of the wave function in the time-modulated region is given by

$$\Psi_{n,\sigma}(x,t) = \exp\left(\eta_\sigma\frac{\alpha_1}{\Omega}\sin\Omega t\frac{\partial}{\partial x}\right)\int d\varepsilon[\tilde{A}_n^\sigma(\varepsilon)e^{ik_{n,R}^\sigma(\varepsilon)x} + \tilde{B}_n^\sigma(\varepsilon)e^{ik_{n,L}^\sigma(\varepsilon)x}]e^{-i\varepsilon t}. \quad \text{(B1)}$$

The matching of the wave functions at all times requires the form $\tilde{F}_n^\sigma(\varepsilon)=\Sigma_{m'}F_n^\sigma(m')\delta(\varepsilon-\mu_n-m'\Omega)$.[15] Hence, the nth-subband scattering wave function is of the form

$$\Psi_{n,\sigma}(x,t) = e^{ik_{n,R}^\sigma(E)x}e^{-iEt} + \sum_m r_{n,LL}^{m,\sigma}e^{ik_{n,L}^{m,\sigma}x}e^{-i(E+m\Omega)t}, \quad \text{if } x<-\frac{l}{2} \quad \text{(B2)}$$

$$\Psi_{n,\sigma}(x,t) = \sum_{m,m'}(-\eta_\sigma)^{m-m'}\left[A_n^\sigma(m')e^{ik_{n,R}^{m',\sigma}x}J_{m-m'}\left(\frac{\alpha_1}{\Omega}k_{n,R}^{m',\sigma}\right) + B_n^\sigma(m')e^{ik_{n,L}^{m',\sigma}x}J_{m-m'}\left(\frac{\alpha_1}{\Omega}k_{n,L}^{m',\sigma}\right)\right]e^{-i(E+m\Omega)t}, \quad \text{if } |x|<\frac{l}{2} \quad \text{(B3)}$$

$$\Psi_{n,\sigma}(x,t) = \sum_m t_{n,RL}^{m,\sigma}e^{ik_{n,R}^{m,\sigma}x}e^{-i(E+m\Omega)t}, \quad \text{if } x>\frac{l}{2}. \quad \text{(B4)}$$

By invoking the boundary conditions in Appendix A, the reflection and the transmission coefficients can all be solved.

[1] *Semiconductor Spintronics and Quantum Computation*, edited by D. D. Awschalom, N. Samarth, and D. Loss (Springer-Verlag, Berlin, 2002).

[2] S. A. Wolf, D. D. Awschalom, R. A. Buhrman, J. M. Daughton, S. von Mohnár, M. L. Roukes, A. Y. Chtchelkanova, and D. M. Treger, Science **294**, 1488 (2001); Y. Kato, R. C. Myers, D. C. Driscoll, A. C. Gossard, J. Levy, and D. D. Awschalom, *ibid.* **299**, 1201 (2003); S. Murakami, N. Nagaosa, and S. C. Zhang, *ibid.* **301**, 1348 (2003).

[3] E. R. Mucciolo, C. Chamon, and C. M. Marcus, Phys. Rev. Lett. **89**, 146802 (2002).

[4] Experimental realization was reported by S. K. Watson, R. M. Potok, C. M. Marcus, and V. Umansky, Phys. Rev. Lett. **91**, 258301 (2003).

[5] Q. F. Sun, H. Guo, and J. Wang, Phys. Rev. Lett. **90**, 258301 (2003).

[6] A. Brataas, Y. Tserkovnyak, G. E. W. Bauer, and B. I. Halperin, Phys. Rev. B **66**, 060404(R) (2002).

[7] P. Zhang, Q. K. Xue, and X. C. Xie, Phys. Rev. Lett. **91**, 196602 (2003).

[8] Y. A. Bychkov and E. I. Rashba, J. Phys. C **17**, 6039 (1984).

[9] J. Nitta, T. Akazaki, H. Takayanagi, and T. Enoki, Phys. Rev. Lett. **78**, 1335 (1997).

[10] D. Grundler, Phys. Rev. Lett. **84**, 6074 (2000).

[11] P. Sharma and P. W. Brouwer, Phys. Rev. Lett. **91**, 166801 (2003).

[12] M. Governale, F. Taddei, and R. Fazio, Phys. Rev. B **68**, 155324 (2003).

[13] A. G. Mal'shukov, C. S. Tang, C. S. Chu, and K. A. Chao, Phys. Rev. B **68**, 23 3307 (2003).

[14] P. F. Bagwell and R. K. Lake, Phys. Rev. B **46**, 15329 (1992).

[15] C. S. Tang and C. S. Chu, Phys. Rev. B **53**, 4838 (1996).

[16] G. Lommer, F. Malcher, and U. Rössler, Phys. Rev. Lett. **60**, 728 (1988).

[17] L. Y. Wang, C. S. Tang, and C. S. Chu (unpublished).